Available at www.sciencedirect.com

ScienceDirect

journal homepage: www.elsevier.com/locate/he

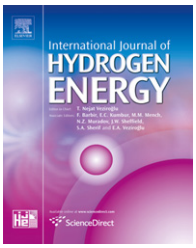

Design of improved fuel cell controller for distributed generation systems

F.A. Olsen Berenguer [a,*], M.G. Molina [b]

[a] Instituto de Energía Eléctrica, Universidad Nacional de San Juan, Av. Libertador San Martín Oeste, 1109, J5400ARL San Juan, Argentina
[b] CONICET, Instituto de Energía Eléctrica, Universidad Nacional de San Juan, Av. Libertador San Martín Oeste, 1109, J5400ARL San Juan, Argentina

ARTICLE INFO

Article history:
Received 28 November 2009
Accepted 17 December 2009
Available online 20 January 2010

Keywords:
Distributed generation (DG)
Fuel cell power plant (FCPP)
Power conditioning system
Three-phase three-level voltage source inverter
High-power isolated DC/DC converter
Control techniques

ABSTRACT

The world has been undergoing a deregulation process which allowed competition in the electricity generation sector. This situation is bringing the opportunity for electricity users to generate power by using small-scale generation systems with emerging technologies, allowing the development of distributed generation (DG). A fuel cell power plant (FCPP) is a distributed generation technology with a rapid development because it has promising characteristics, such as low pollutant emissions, silent operation, high efficiency and long lifetime because of its small number of moving parts. The power conditioning system (PCS) is the interface that allows the effective connection to the electric power system. With the appropriate topology of the PCS and its control system design, the FCPP unit is capable of simultaneously performing both instantaneous active and reactive power flow control. This paper describes the design and implementation of a novel high performance PCS of an FCPP and its controller, for applications in distributed generation systems. A full detailed model of the FCPP is derived and a new three-level control scheme is designed. The dynamic performance of the proposed system is validated by digital simulation in SimPowerSystems (SPS) of MATLAB/Simulink.

© 2009 Professor T. Nejat Veziroglu. Published by Elsevier Ltd. All rights reserved.

1. Introduction

The management of global energy resources is increasingly becoming a problem for the future of humanity. If energy demand is maintained at today's levels, there will be just a few generations left before the collapse of fossil fuel reserves. Worldwide, utilization of non-renewable energy sources has been dominant for several years. Nowadays, a high percentage of the installed generation capacity comes from power plants operated with hydrocarbons, such as coal, fuel oil and natural gas. This combustion-based technology causes the emission of polluting gases that are aggressive for health and the environment [1].

The need to find new energy solutions is obviously driven by the concern over increasing pollution and greenhouse gas emissions, rapidly declining fuel reserves and also to extend the lifetime of finite fossil fuels [2]. These problems, far from finding effective solutions, are continuously increasing, which causes the necessity of technological alternatives to assure, on one hand the appropriate supply and quality of the electric power and on the other one, the saving and the efficient use of the natural resources preserving the environment.

An alternative technological solution to help this problem is the use of small generation units and their integration into the distribution system as near as possible to the consumption site, permitting to improve the power quality and

* *Corresponding author*. Tel.: +54 264 4226444; fax:+54 264 4210299.
E-mail address: faolsenberenguer@gmail.com (F.A. Olsen Berenguer).
0360-3199/$ – see front matter © 2009 Professor T. Nejat Veziroglu. Published by Elsevier Ltd. All rights reserved.
doi:10.1016/j.ijhydene.2009.12.097

reliability of the electric power generation. This solution is known as distributed or dispersed generation (DG) and promotes the development of clean non-conventional technologies of generation that use renewable energy sources (RESs) that do not cause environmental pollution, such as wind, photovoltaic, hydraulic, biomass, among others [2,3].

A fuel cell (FC), as a renewable energy source, is considered one of the most promising sources of electric power. An FC is an electrochemical device that oxidizes the fuel (without combustion) to directly transform the chemical energy of the fuel into electrical energy. With a low environmental impact, operating practically silently, with high efficiency and long lifetime because of its small number of moving parts, fuel cells represent a very good option as a DG unit in the future of electricity generation markets [4].

The main components of an FC power plant (FCPP) include the fuel processing unit or reformer, the fuel cell stack, and the power conditioning system (PCS). The PCS is the interface that allows the effective connection to the electric system. With the appropriate topology of the PCS and its control system design, the FC unit is capable of simultaneously performing both instantaneous active and reactive power flow control.

This paper describes the design and implementation of a novel high performance PCS of an FCPP and its controller, for applications in distributed generation systems. A full detailed model of the FCPP is derived, including the FC stack and two power converters to provide the high-efficiency PCS capability, as depicted in Fig. 1. Main commercially available fuel cells are modeled, including proton exchange membrane (PEMFC) and solid oxide (SOFC) fuel cells. The PCS consists of a three-phase three-level AC/DC converter and incorporates a high-power isolated DC/DC converter as interface with the FC stack. Moreover, based on the state-space averaging method a three-level control scheme is designed, comprising a full decoupled current control strategy in the synchronous-rotating d–q reference frame with a novel controller to prevent the voltage drift/imbalance of the AC/DC converter DC bus capacitors. The dynamic performance of the proposed system is validated by digital simulation in SimPowerSystems (SPS) of MATLAB/Simulink.

2. Detailed modeling of the FCPP

2.1. *Fuel cell unit*

A fuel cell is an energy conversion system that theoretically has the capacity to produce as much energy as fuel and oxidant are provided to the electrodes [5]. Fig. 1 (bottom right side) shows the basic structure of the fuel cell unit. The process happens in a natural way, caused by the need of charged particles to move to low electrochemical energy regions. Charged particles of hydrogen move towards oxygen and join with it because oxygen particles have low electrochemical energy. The movement of these charged particles

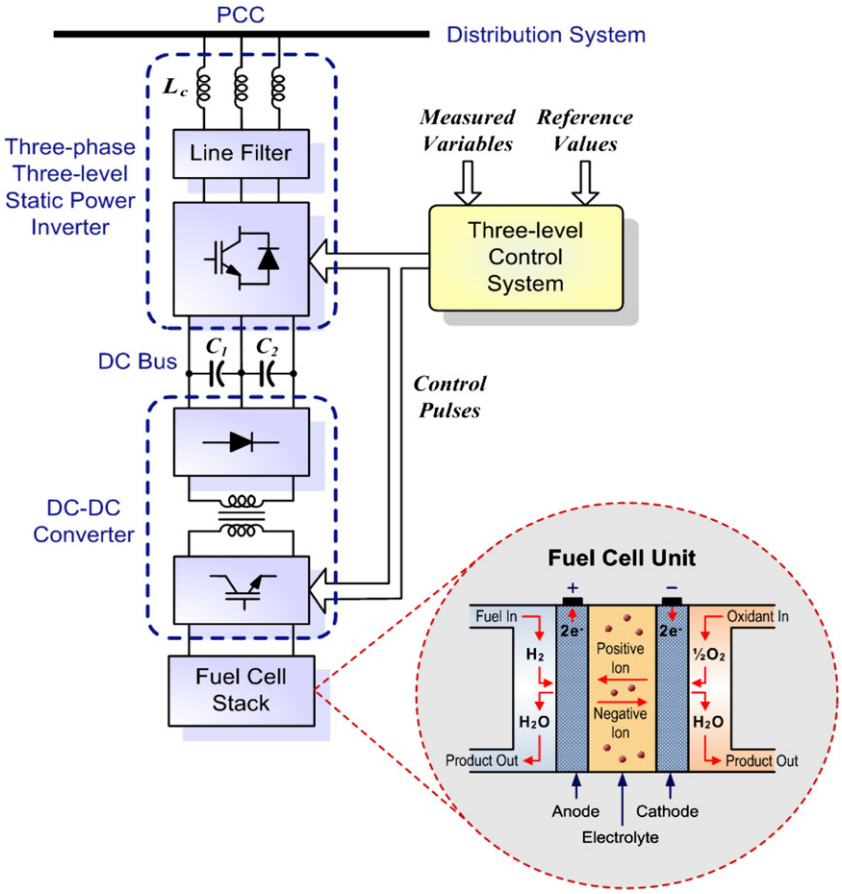

Fig. 1 – General scheme of a fuel cell power plant.

can be used to generate electrical energy, which is in essence a controlled movement of electrons. When hydrogen and oxygen are separated by an electrolyte (electrolytic membrane) an interesting and useful process takes place. The protons of the hydrogen atoms move through the membrane but the electrons cannot do that. These electrons try to move to the other side of the membrane to achieve a stable state. When an electrical circuit is connected between both electrodes, the electrons travel through it. This movement of electrons through the external electrical circuit is controlled to generate electrical energy [6].

In the electrochemical process, the total reaction is divided into two small reactions, one of them is an oxidation reaction and the other one is a reduction reaction. The oxidation reaction starts with the dissociation of hydrogen atoms into protons and electrons and takes place at the anode. This reaction is represented by Eq. (1).

$$H_2 \rightarrow 2H^+ + 2e^- \tag{1}$$

Once the protons have passed through the electrolyte and the electrons flowed along the external circuit to the cathode, a reduction reaction happens, where the protons and electrons of hydrogen recombine to form water, as shown in Eq. (2).

$$1/2O_2 + 2H^+ + 2e^- \rightarrow H_2O \tag{2}$$

This means that the global reaction of the fuel cell is represented by:

$$H_2 + 1/2O_2 \rightarrow H_2O \tag{3}$$

The efficiency of this process depends mainly on the capacity of the electrolyte to create the necessary chemical reactivity for carrying ions, and thus of the type of electrolyte employed [7]. The general design of most fuel cells is similar except for the electrolyte. The five main types of FCs, as defined by their electrolyte, are alkaline fuel cells (AFC), proton exchange membrane fuel cells (PEMFC), phosphoric acid fuel cells (PAFC), molten carbonate fuel cells (MCFC), direct methanol fuel cells (DMFC), and solid oxide fuel cells (SOFC). In this work, two types of FCs are analyzed, PEMFC and SOFC.

The FCPP consists of three basic components: a fuel reformer or processor, a power section, and a power conditioner. The reformer or processor extracts pure hydrogen (H_2) from hydrocarbon fuels such as natural gas, methanol or coal for use in the FC unit. The power section is where H_2 and O_2 are combined in order to generate electricity and waste heat. The PCS is the power electronics that converts DC power generated by the FC to AC power.

The detailed model of the FC unit is based on Refs. [6–8] and simulates the relationship between output voltage and partial pressure of hydrogen, oxygen and water. To this end, the following main assumptions have been made: (*i*) the fuel cell gases are ideal; (*ii*) it is sufficient to define only one single pressure value inside the electrodes; (*iii*) the fuel cell temperature is stable at all times; and (*iv*) Nernst's equation is used to determine the voltage between the terminals.

The main equations describing the dynamics response of the FC power section can be generalized for both PEMFC and SOFC as follows:

$$\dot{p}_{H_2} = \frac{1}{\tau_{H_2}}\left(\frac{1}{K_{H_2}}\left(q_{H_2} - 2K_r I_{fc}\right) - p_{H_2}\right) \tag{4}$$

$$\dot{p}_{H_2O} = \frac{1}{\tau_{H_2O}}\left(\frac{2K_r}{K_{H_2O}} I_{fc} - p_{H_2}\right) \tag{5}$$

$$\dot{p}_{O_2} = \frac{1}{\tau_{O_2}}\left(\frac{1}{K_{O_2}}\left(\frac{1}{r_{H-O}} q_{H_2} - K_r I_{fc}\right) - p_{H_2}\right) \tag{6}$$

where I_{fc} is the fuel cell current; q_{H_2} stands for the hydrogen input flow; p_{H_2}, p_{O_2}, p_{H_2O} denote the partial pressures of hydrogen, oxygen, and water, respectively. The time constants τ_{H_2}, τ_{H_2O}, τ_{O_2}, designate the response times of hydrogen, water, and oxygen flows, respectively. K_{H_2}, K_{H_2O}, and K_{O_2}, denote the valve molar constants for hydrogen, water and oxygen.

The SOFC is characterized by high operating temperatures, use of ceramic electrolyte and the absence of external reformer, while the PEMFC employs low working temperature and an external reformer to convert methane into H_2 by steam reforming. Thus, in order to develop a full detailed mathematical model describing both FC dynamics, a configurable topology by switches is proposed, as described in Fig. 2.

The SOFC model is obtained by setting S_1 through S_3 at position H (high). In this case, the dynamic response of the H_2 processor is related to the time that takes to change the chemical parameters of the reaction after a change in the fuel flow. This response is modeled by a first order transfer function with a time constant τ_f. In the same way, the dynamic response of the FC current, which is generally fast, is also modeled by a first order transfer function with a time constant τ_e. Oxygen flow is determined using the hydrogen–oxygen flow ratio r_{H-O}.

The PEMFC model is obtained by setting S_1 through S_3 at position L (low). In this case, a simple model of the reformer that generates H_2 through reforming methane is used. This model is a second-order transfer function with reformer time constants τ_1, τ_2, conversion factor CV, and reference methane flow rate q_{methr}. In order to control hydrogen flow according to the output power from the fuel cell, a feedback from the FC current is considered. A proportional integral (PI) controller is used to control the flow rate of methane in the reformer, $k3$ and $\tau 3$ being the PI gain and time constants. As with previous FC, oxygen flow is determined using the hydrogen–oxygen flow ratio r_{H-O}. The reformer and its controller are illustrated in Fig. 2 (left bottom side), where N_0 is the number of series of FCs in the stack, F is Faraday's constant and U is the fuel utilization factor.

Nernst's equation represents the voltage between the terminals of the fuel cell. It determines the efficiency of the fuel cell by means of a comparison between the standard ideal voltage (E_0) and the voltage considering the effects of temperature and partial pressure of the reactants.

$$V_{fc} = N_0\left(E_0 + \frac{RT}{2F}\log\left(\frac{p_{H_2}\sqrt{p_{O_2}}}{p_{H_2O}}\right)\right) - B\ln(CI_{fc}) \tag{7}$$

where R is the universal gas constant, T is the absolute temperature, B and C are constants that consider the activation overvoltage in PEMFCs.

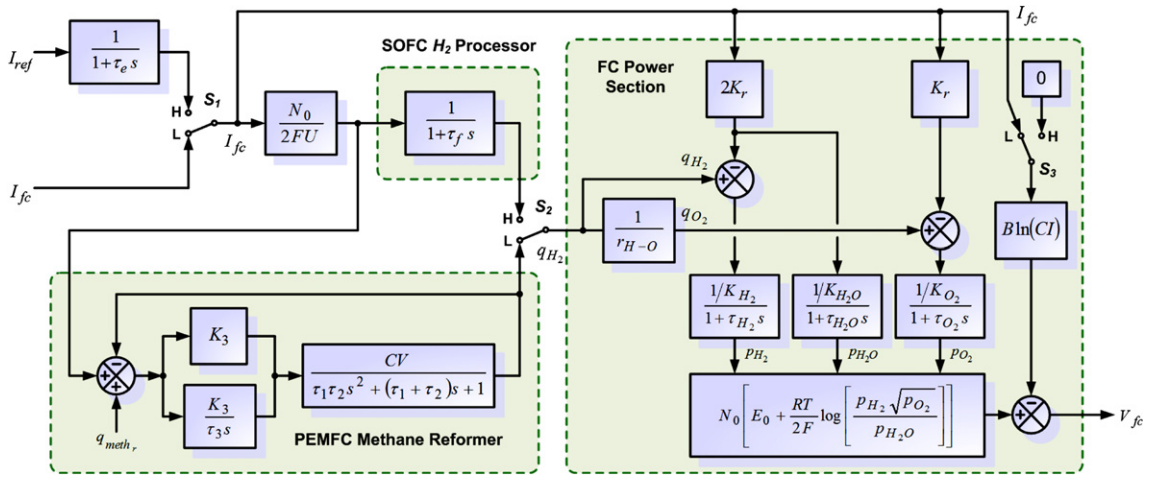

Fig. 2 – Model of the FCPP power section and fuel processor.

2.2. *Power conditioning system*

Fig. 3 summarizes the proposed detailed model of the FCPP for applications in distributed generation systems. This model consists of the FC model previously developed and the PCS for connection to the electric grid. The PCS is made up of the voltage source inverter (VSI) and the DC/DC converter to interface the VSI with the FC.

The power conditioning system used for connecting RESs to the distribution grid requires flexible, efficient and reliable generation of high quality electric power [9]. In order to obtain a high performance compensation device for high current applications of grid-connected FCPPs, the PCS must be carefully designed, especially due to the limited ratings of the available semiconductors. The PCS proposed in this work is composed of a two-stage high performance topology that fulfills all the requirements stated above.

A three-phase three-level VSI using high-speed high-power insulated gate bipolar transistors or IGBTs is employed for connecting the fuel cell to the electric grid, as described in Fig. 3 (right side). The VSI corresponds to a DC/AC converter controlled through sinusoidal pulse width modulation (SPWM) techniques. The inverter structure is based on a diode-clamped three-level topology, also called neutral point clamped (NPC), instead of a standard two-level six-pulse inverter structure. This three-level twelve-pulse VSI topology generates a more smoothly sinusoidal output voltage waveform than conventional structures without increasing the switching frequency and effectively doubles the power rating of the VSI for a given semiconductor device, which is very significant for high-power FC applications. The connection to the utility grid is made through a coupling reactor and a low pass filter in order to reduce the perturbation on the distribution system from high-frequency switching harmonics generated by the PWM control. In this way, the harmonic performance of the inverter is improved, also obtaining better efficiency and reliability with respect to the conventional two-level inverter topology.

This inverter topology can be applied to reactive power generation almost without voltage imbalance problems. But when active power exchange is included, as is the case with an FCPP, the AC/DC converter could not have balanced voltages without sacrificing output voltage performance and auxiliary converters would be needed in order to provide a compensating power flow between the capacitors of the DC link. For this reason, the use of an advanced high-power DC/DC converter as interface between the VSI and the FC is required, instead of a standard one. To this aim, this paper proposes an efficient, parallel–series full bridge (P–SFB) inverter topology derived from Ref. [10], composed of two IGBT full-bridge voltage-fed inverters (FBs) operating with a high transmission ratio transformer and uncontrolled full-wave

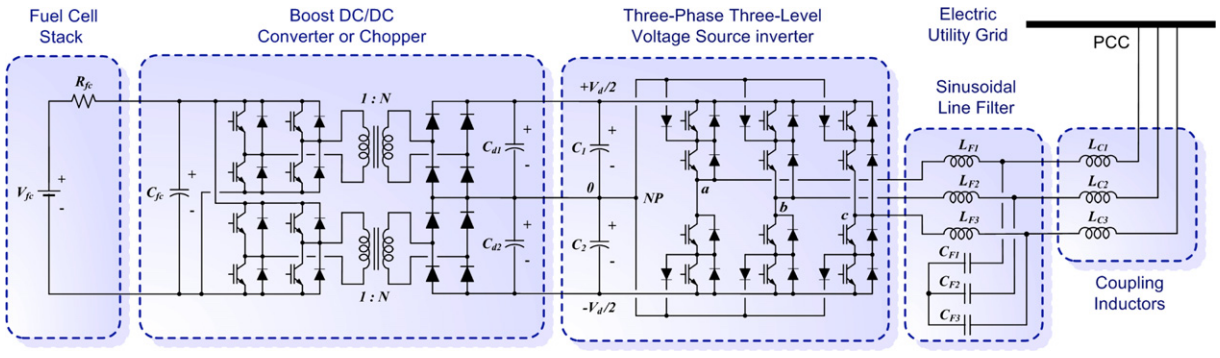

Fig. 3 – Full detailed model of the proposed fuel cell power plant.

rectifier bridge, as shown in Fig. 3 (upper left side). The two conventional FB converters are connected in parallel at the DC input side (FC side) and in series at the rectifier output (VSI side). In this way, the device permits to increase the chopper power ratings while maintaining high dynamic performance and decreasing the harmonics distortion produced. Furthermore, the compact high-frequency isolation transformer provides safety decoupling of the FC from the AC system.

Phase shifting modulation is used to regulate the output voltage of both FB converters. Each bridge operates at the same switching frequency and leg-to-leg phase shift to generate half of the output power. Since both FB converters are series-connected at the output and then shunt-connected to the DC bus capacitors of the VSI, this work proposes an independent duty cycle control of each FB converter so as to maintain the charge balance of the DC bus capacitors, thus avoiding contributing to the AC system with additional distortion.

3. Proposed control strategy of the FCPP

The proposed control of the three-phase grid-connected FCPP consists of an external, middle and internal level, as depicted in Fig. 4.

3.1. External level control

The external level control (left side of Fig. 4) is responsible for determining the active and reactive power exchange between the FCPP and the utility grid. This control scheme is designed for performing two major control objectives: the voltage control mode (VCM) for ride-through voltage fluctuations and the active power control mode (APCM) for dynamic active power exchange with the electric grid.

The VCM is designed to control the voltage at the PCC of the VSI, through the modulation of the reactive component of the output current (fundamental quadrature component, i_{qr1}). To this aim, the magnitude of the voltage vector at the PCC (v_{d1}) is compared to a voltage reference. An error signal is produced and then fed to a proportional integral (PI) controller with a regulation droop R_d.

The APCM allows controlling the active power exchange between the FCPP and the utility grid by means of the boost DC/DC converter. This control mode compares the reference power set by an external input with the actual measured value computed as $v_{d1}\, i_{d1}$, in order to eliminate the steady-state in-phase output current component of the power electronic device via a PI compensator. In this way, the active power flow between the FCPP and the power system can be controlled so as to force the FC to inject the active power P_r, thus operating as a DG system.

3.2. Middle level control

The middle level control makes the actual active and reactive power exchange between the FCPP and the AC system, to dynamically track the reference values set by the external level. The middle level control design, which is depicted in Fig. 4 (middle side of Fig. 4), is based on a linearization of the state-space averaged mathematical model of the VSI in d–q coordinates described in Ref. [11]. The dynamics equations governing the instantaneous values of the three-phase output voltages in the AC side of the VSI and the current exchanged with the utility grid can be derived in the dq reference frame as follows:

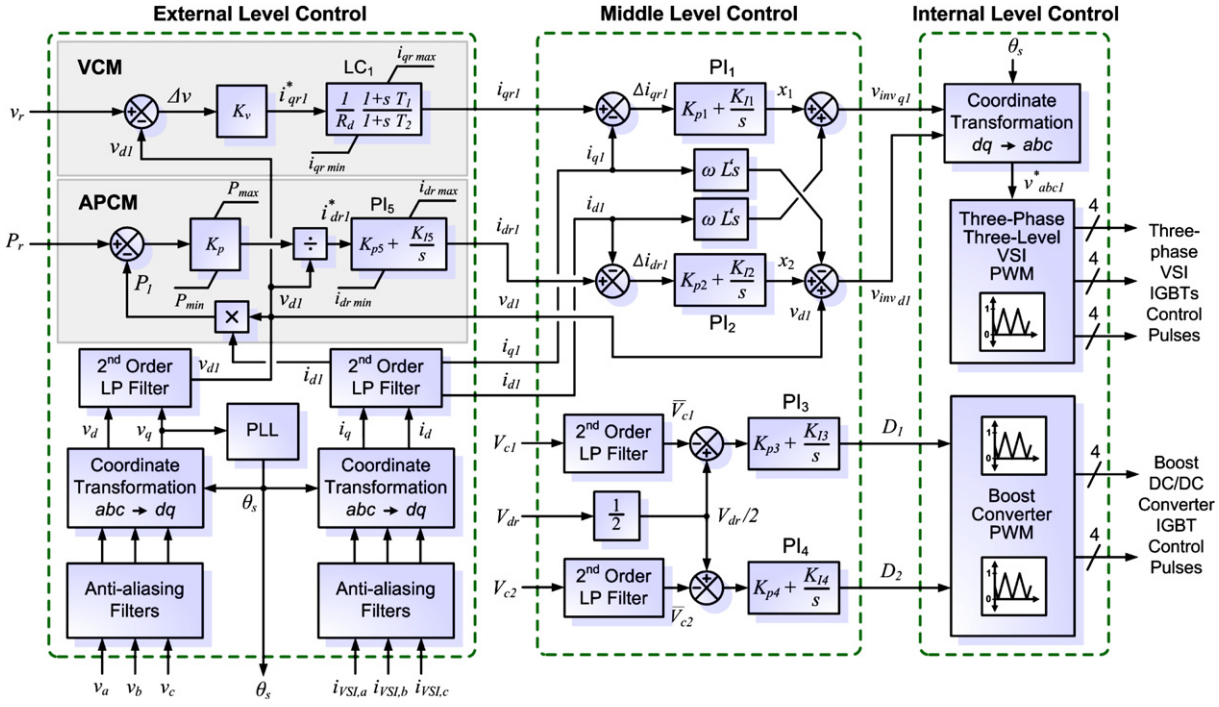

Fig. 4 – Proposed multi-level control scheme for the three-phase grid-connected FCPP.

$$s\begin{bmatrix} i_d \\ i_q \\ V_d \end{bmatrix} = \begin{bmatrix} \frac{-R_s}{L_s} & \omega & \frac{mS_d}{2L_s} \\ -\omega & \frac{-R_s}{L_s} & \frac{mS_q}{2L_s} \\ \frac{-3}{2\ C_d}mS_d & \frac{-3}{2\ C_d}mS_q & \frac{-2}{R_pC_d} \end{bmatrix} \begin{bmatrix} i_d \\ i_q \\ V_d \end{bmatrix} - \begin{bmatrix} \frac{v}{L_s} \\ 0 \\ 0 \end{bmatrix} \quad (8)$$

where,

$s = d/dt$: Laplace variable, defined for $t > 0$.
ω: synchronous angular speed of the grid voltage at the fundamental frequency.
m: modulation index of the VSI, $m_i \in [0, 1]$.
R_s: equivalent resistance accounting for the coupling inductors resistance and VSI semiconductors conduction losses.
L_s: equivalent inductance of the coupling inductors.
C_d: equivalent capacitance of the DC bus capacitors.
R_p: equivalent resistance representing the VSI semiconductors switching losses and power loss in both DC bus capacitors.
$S_d = \cos\alpha$, $S_q = \sin\alpha$: average switching factors of the VSI in the dq frame, and α the phase shift of the VSI output voltage from the reference position.

Inspection of Eq. (8) shows a cross-coupling of both components of the VSI output current through ω. Therefore, in order to achieve a fully decoupled active and reactive power control, it is simply required to decouple the control of i_d and i_q through two conventional PI controllers, as depicted in Fig. 4. In addition, it can be seen from Eq. (8) the additional coupling resulting from the DC capacitors voltage V_d, as much in the DC side (lower part) as in the AC side (upper part). This difficulty demands maintaining the DC bus voltage as constant as possible through extra PI compensators which allows eliminating the steady-state voltage variations at the DC bus, by forcing the instantaneous balance of power between the DC and the AC sides of the VSI through the control of the duty cycle $D = (D_1 + D_2)$ of the DC/DC chopper. Finally, duty cycles D_1 and D_2 are independently computed through a novel controller in order to prevent DC bus capacitors' voltage drift/imbalance. This extra DC voltage control provides the availability of managing D_1 and D_2 according to the capacitors' charge imbalance. In this way, this condition greatly reduces instability problems caused by harmonics as much in the VSI as in the AC system.

3.3. *Internal level control*

The internal level (right side of Fig. 4) is responsible for generating the switching signals for the twelve IGBTs of the three-level VSI, and for the eight IGBTs of the boost DC/DC converter. This level is mainly composed of a line synchronization module, a three-phase three-level SPWM firing pulse generator and a PWM pulse generator for the chopper.

4. Digital simulation results

In order to investigate the effectiveness of the proposed models and control algorithms, digital simulations were implemented using SPS of MATLAB/Simulink [12]. For validation of both control strategies, i.e. APCM and VCM, two sets of simulations were carried out. The numerical values of the SOFC and PEMFC constants are derived from Ref. [8].

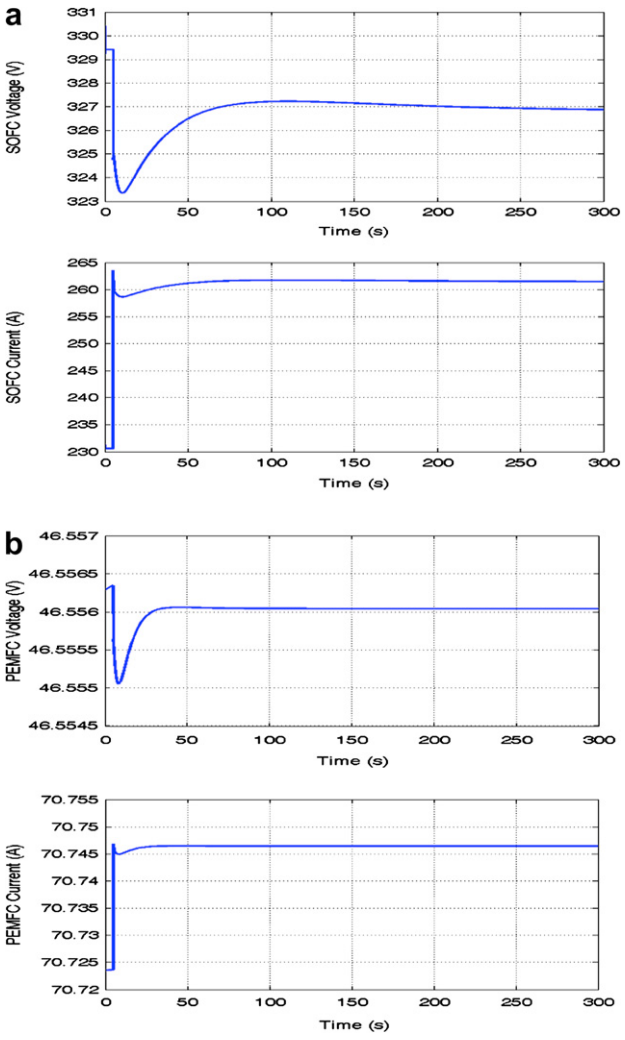

Fig. 5 – Dynamic response of the proposed FC controller in active power control (APCM). (a) SOFC. (b) PEMFC.

Simulations depicted in Fig. 5 show the case with only active power exchange with the utility grid, i.e. with just the APCM activated, for the FCPP connected to the AC system. To this aim, the power generated by a 100 kW SOFC is commanded to provide a step change at $t = 5$ s so that the dynamic performance can be studied. Fig. 5a shows the voltage transient response for a sudden increase in the demanded power of about 0.1 p.u. when the fuel cell plant is operating in steady state at 0.75 p.u. It can be seen that during the first 10 s after the power step, the voltage descends rapidly because the reactants at the electrodes are consumed and the large time constants of the chemical reactions in the cells avoid the hydrogen and oxygen to refill the electrodes. At that point, the fuel reformer is already able to give the necessary hydrogen and oxygen to the electrodes to elevate their partial pressures and the fuel cell output voltage. With an H_2O time constant of 78.3 s, the

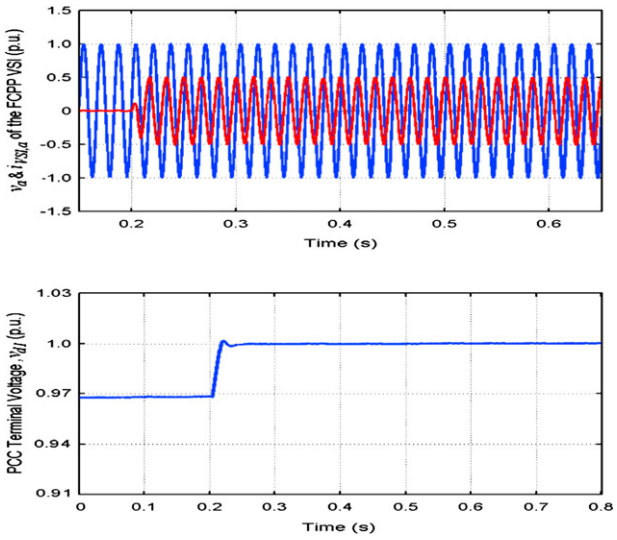

Fig. 6 – Dynamic response of the proposed SOFC controller in voltage control mode (VCM).

voltage transient response for this SOFC is very slow, as can be observed. In the case of the current, initially, it follows the load step and seems to reach its steady-state value faster than the voltage, without important variations in its value. Now, the same load step of about 0.1 p.u. at $t = 5$ s is applied to a 5 kW PEMFC, operating in steady-state at 0.7 p.u. Fig. 5b shows a faster transient response when comparing to the one of the SOFC. There is also a voltage drop that lasts until the fuel reformer and the internal chemical reactions allow the fuel and oxidant to react.

Simulations of Fig. 6 show the case with only reactive power exchange with the utility grid for the FCPP connected to the AC system, i.e. the APCM is deactivated all the time while the VCM is activated at $t = 0.2$ s after the SOFC is in steady-state, i.e. after 200 s. As can be seen, the rapid injection of reactive capacitive power into the electric system when the VCM is activated allows quick regulation of the PCC voltage at 1 p.u. The instantaneous phase 'a' voltage at the PCC is 90° phase-shifted in lag with respect to the FCPP VSI output current during the reactive power injection, thus verifying the only capacitive generation with no active power exchange. This reactive power exchange effectively influences the terminal voltage v_{d1}, as can be observed.

5. Conclusion

A novel power conditioning system of an FCPP to simultaneously and independently control active and reactive power flow in distributed generation systems, and its controller has been studied and implemented in this paper. The use of a three-phase three-level voltage source inverter coupled with an isolated boost DC/DC converter as interface with the FC, allows exchanging active power and implementing an effective balancing technique of the DC link capacitors. Moreover, a real detailed full model of the FCPP and a new three-level control scheme have been proposed. The dynamic performance of the proposed systems has been fully validated by digital simulations.

REFERENCES

[1] Willis HL, Scott WG. Distributed power generation – planning and evaluation. New York: Marcel Dekker; 2000.
[2] El-Khattam W, Salama MMA. Distributed generation technologies, definitions and benefits. Electric Power Systems Research Oct 2004;71(2):119–28.
[3] Rahman S. Going green: the growth of renewable energy. IEEE Power and Energy Magazine Nov/Dec 2003; 1(6):16–8.
[4] Vielstich W, Lamm A, Gasteiger H. Handbook of fuel cells: fundamentals, technology applications. 4-Volume Set. John Wiley and Sons; May 2003.
[5] Smith JA, Nehrir MH, Gerez V, Shaw SR. A broad look at the workings, types, and applications of fuel cells. In: IEEE/PES 2002, Power Engineering Society summer meeting records; July 2002. p. 70–5.
[6] El-Sharkh M, Rahman A, Alam M, Sakla A, Byrne P, Thomas T. Analysis of active and reactive power control of a stand-alone PEM fuel cell power plant. IEEE Transactions on Power System Nov 2004;19(4):2022–8.
[7] Kandepu R, Imsland L, Foss BA, Stillerc C, Thorudc B, Bolland O. Modeling and control of a SOFC-GT-based autonomous power system. Energy 2007;32(4):406–17.
[8] González-Longatt F, Facendo A, Peraza C, Villanueva C. Caracterización de la Operación de Celdas de Combustible como Fuente de Generación de Electricidad. In: Congreso Venezolano de Redes y Energía Eléctrica Records; Nov 2007. p. 1–13.
[9] Carrasco JM, Garcia-Franquelo L, Bialasiewicz JT, Galván E, Portillo-Guisado RC, Martín-Prats MA, et al. Power electronic systems for the grid integration of renewable energy sources: a survey. IEEE Transactions on Industrial Electronics August 2006;53(4):1002–16.
[10] Wang Y, Choi S, Lee E. Fuel cell power conditioning system design for residential application. International Journal of Hydrogen Energy 2009;34(5):2340–9.
[11] Molina MG, Mercado PE. Control design and simulation of DSTATCOM with energy storage for power quality improvements. In: IEEE/PES 2006 records, transmission and distribution conference and exposition: Latin America; August 2006. p. 1–8.
[12] The MathWorks Inc. SimPowerSystems for use with Simulink: user's guide, updated for Simulink v7.3 (release 2009a). Available at. <www.mathworks.com>; 2009.